4-2015

pH dependence of DNA binding of DNA Polymerase 1Klenow-like fragments from D. radiodurans, T. aquaticus,and .E coli

Katelyn Jackson

pH dependence of DNA binding of DNA Polymerase I Klenow-like fragments from *D. radiodurans*, *T. aquaticus*, and *E. coli*

by

Katelyn Jackson

Undergraduate honors thesis under the direction of

Dr. Vince LiCata

Department of Biological Sciences

Submitted to the LSU Honors College in partial fulfillment of

the Upper Division Honors Program.

April, 2015

Louisiana State University

& Agricultural and Mechanical College

Baton Rouge, Louisiana

pH dependence of DNA binding of DNA Polymerase I Klenow-like fragments from *D. radiodurans*, *T. aquaticus*, and *E. coli*

Abstract

Thermus aquaticus and *Deinococcus radiodurans* are both extremophilic organisms that are evolutionarily closely related, but have adapted to different environmental stressors. *T. aquaticus* is a thermophile, and lives in aqueous environments at temperatures approaching 90°C. In contrast, *D. radiodurans* is easily killed at high heat, but is resistant to prolonged desiccation and is one of the most radiation resistant organisms yet identified on Earth. I have comparatively examined the pH dependence of the DNA binding of the large fragment domains of the Pol I DNA polymerases from *T. aquaticus*, *D. radiodurans*, and *E. coli* denoted "Klentaq", "Klendra", and "Klenow", respectively. None of these polymerases shows an unusually strong pH dependence, but the effect of pH on Klendra is significantly greater than on Klentaq or Klenow for both double-stranded (ds) and primed-template (pt) DNA. For Klendra, thermodynamic linkage analysis reports an uptake of 1.5 protons upon binding of ptDNA, and 1 proton upon binding of dsDNA. In contrast, for Klentaq, ptDNA binding is linked to the uptake of only 0.3 protons, while dsDNA binding results in a 0.6 proton uptake. Klenow displayed a proton uptake of 0.35 when binding dsDNA and an uptake of 0.25 protons when binding ptDNA. Thus, the pH linkage is consistently higher for Klendra polymerase, and the relative order of pH sensitivity for the two substrates switches between Klendra and Klentaq (ptDNA > dsDNA for Klendra, dsDNA > ptDNA for Klentaq). The more pronounced protonation linkage for Klendra DNA binding may be related to the widely held hypothesis that the internal pH of *D. radiodurans* decreases during radiation damage. At lower

pH's, the DNA polymerase would bind more tightly to DNA, and Pol I polymerase is known to be essential for the recovery of *D. radiodurans* from radiation damage.

Table of Contents

List of Tables

List of Figures

Introduction

The objective of this project is to compare the stability and binding activity of the Pol I DNA polymerases from two different, but closely related, extremophilic organisms, *Deinococcus radiodurans* DNA polymerase I Klenow-type fragment, hereafter referred to as "Klendra", and the DNA polymerase I Klenow-type fragment from *Thermus aquaticus*, which is called "Klentaq". For comparison, the binding of the DNA polymerase I from mesophilic *E. coli,* "Klenow", was also studied. This study reports the binding thermodynamics of these three proteins as a function of solution pH.

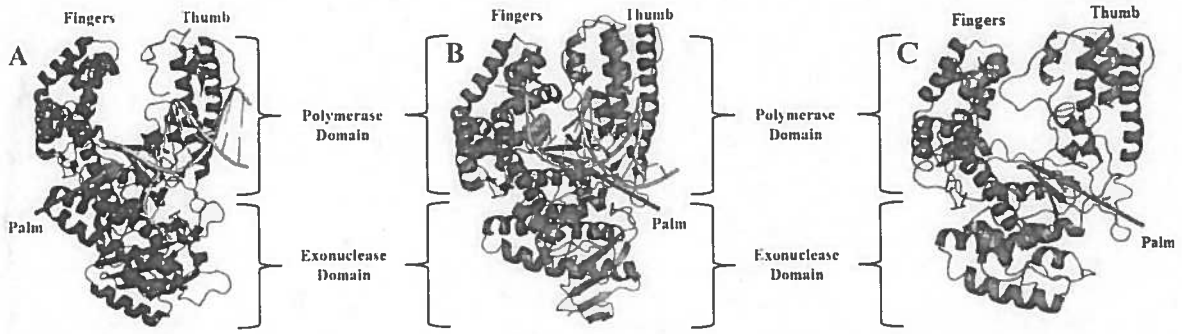

Figure 1: Structures of the Klenow-like fragments Klenow, Klentaq, and Klendra. (A) Crystal structure of Klenow bound to duplex DNA (PDB file 1KLN) (4). (B) Crystal structure of Klentaq bound to duplex DNA and a nucleotide, shown in green (PDB file 4KTQ) (5). (C) SWISS-MODEL predicted structure of Klendra (6). Each domain and subdomain is labeled. Panels A and B by Jaycob Warfel (3).

In vivo, DNA Polymerase I serves important functions in DNA excision repair and DNA replication of the lagging strand by filling in Okazaki fragments. The Klenow fragment of DNA Polymerase I is a fully functional polymerase which contains three active site domains: the catalytic "palm" domain, the "fingers," and the "thumb" domains. Full length DNA Polymerase I also includes the 5'-3' polymerase region and the 3'-5' exonuclease region, but the 5'-3'

exonuclease region is deleted from the Klenow fragment. Originally, the *E. coli* Klenow fragment was formed by enzymatic cleavage at the subtilisin cleavage site between the two nuclease domains, but the current norm is to express Klenow fragments recombinantly. The Klenow construct is often used *in vitro* for DNA synthesis reactions (7). This study characterizes the binding of the DNA polymerase I Klenow-like fragments of *Deinococcus radiodurans* and *Thermus aquaticus*, which are called Klendra and Klentaq, respectively.

Klendra, like other Pol I family polymerases, is not only involved in replication of DNA, it also functions in DNA repair (8). Since the protein itself must also withstand the harsh conditions tolerated by the bacterium *in vivo*, it would seem likely for Klendra itself to be an extremely stable protein, but *in vitro*, purified Klendra has proven to be relatively unstable and difficult to work with. At pH values between 7 and 8, Klendra is barely more thermostable than *E. coli*'s Klenow (3), unlike its closely related homologue Klentaq (9). Klentaq is an interesting comparison protein, because it is from within the same bacterial genus as Klenow and is an extremely stable protein which can retain activity in a variety of pH and salt conditions (9). Identifying the optimal pH and salt levels for Klendra will help determine if the optimal functional conditions for Klendra differ from its Klentaq and Klenow homologues.

Deinococcus radiodurans and *Thermus aquaticus* are both extremely rugged bacterial species. *D. radiodurans* is highly tolerant to both desiccation and radiation. Its radioresistance is thought to be due to its ability to efficiently repair the resulting damage to its genome. Though originally placed in different clades phylogenetically, the *Thermus* and *Deinococcus* groups have been combined into the same group called *Deinococcus-Thermus* (See Figure 2). Members of this group have the ability to survive in extreme conditions, such as radiotoxicity, desiccation, low temperatures and high heat (2).

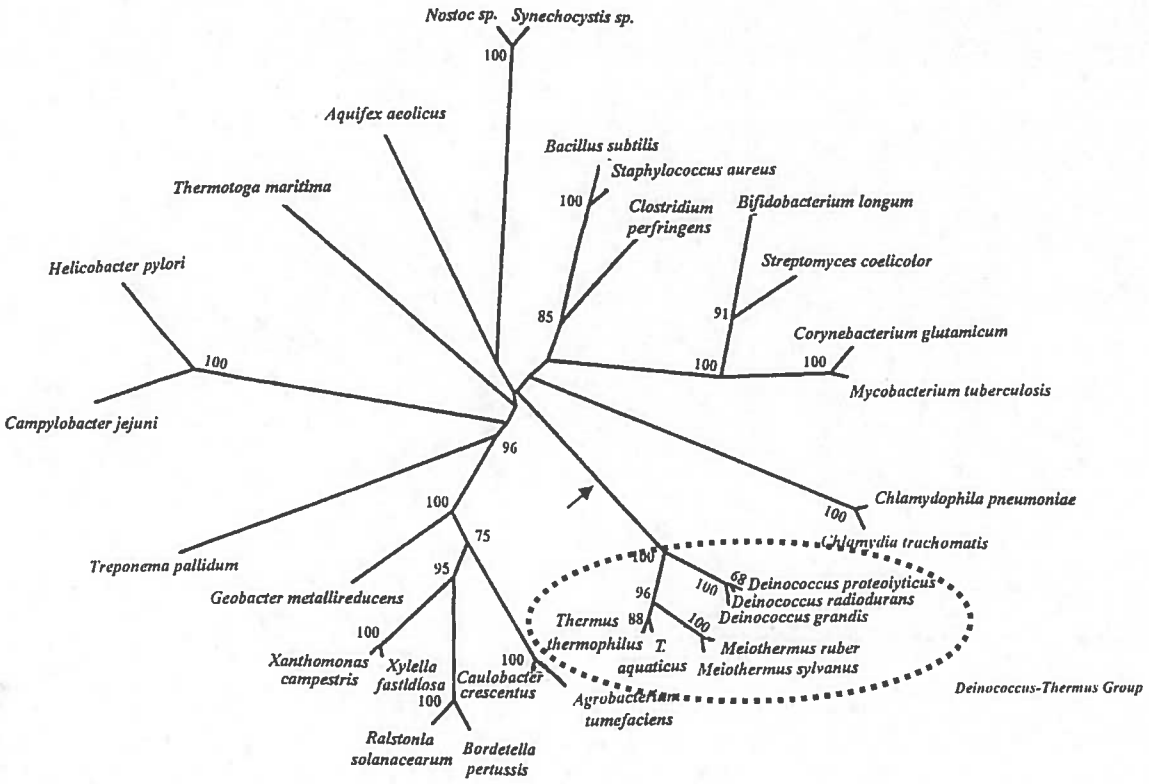

Figure 2: The phylogenetic relationship between *D. radiodurans* and *T. aquaticus*. The combined *Thermus-Deinococcus* group is well-supported by genomic evidence, as shown by the boot-strapping probability values on the branches of the phylogenetic tree. The closer the boot-strapping value is to 100, the better the branch relationship is supported by the genomic alignment. Figure from Griffiths, et al. 2004 (2).

The comparison between Klendra and Klentaq is important because these proteins are closely evolutionarily related and are functionally homologous, but their source organisms, *D. radiodurans* and *T. aquaticus* respectively, come from very different environments. I want to see how closely related the isolated proteins are at a functional level. I will also compare my results with Klenow, from *E. coli*, a mesophilic bacteria, for two reasons. Firstly, it is currently the best characterized polymerase protein. Secondly, because *E. coli* is not adapted to extreme environments; so if a particular pH dependence is an adaptation to cope with extreme

environments, Klenow should not exhibit the same pH linkage as Klendra and Klentaq over the same pH ranges, as will be discussed later in this thesis. As will also be later discussed, pH dependence of binding could be an advantageous adaptation for Klendra if the intracellular pH of the cell drops upon irradiation.

Ever since the earliest characterizations of *E. coli* Polymerase I by Kornberg and by Benkovic, polymerase-DNA binding titrations have been typically performed at about pH 7.9 (10,11). However, initial DNA binding titrations with Klendra at pH 7.9 were inconsistent and indicated very weak binding compared with other characterized Pol I polymerases (3). Klentaq and Klenow have not presented such problems at pH 7.9. Therefore, the DNA binding of Klendra polymerase was charactarized as a function of pH.

Materials and Methods

2.1.1: Materials

DNA ligand.

The following DNA substrates were obtained from IDT: 5' ROX (carboxy-X-rhodamine)-labeled 13mer, unlabeled 20mer, 5' ROX-labeled 20mer. 5' ROX-labeled 20mer and unlabeled 20mer were annealed to form 20/20mer dsDNA. 5' ROX-labeled 13mer (primer strand) and unlabeled 20mer (template strand) were annealed to form 13/20mer ptDNA. ROX is a fluorophore that is conjugated to a nucleotide on the 5' end of the nucleotide strand via an ester linkage. The 5' nucleotide has been modified to have an amino group that will form the ester linkage with the ROX label. ROX has an extinction max at 588 nm and an emission max at 608 nm (IDT). The sequences of the DNA fragments are shown in Table 2, below.

Table 1: Sequences of ROX-labeled DNA substrates for polymerase binding experiments. This table contains the sequences for each DNA substrate type. An asterisk (*) denotes the ROX-label attachment site.

Substrate	Sequence
PT 13/20mer	5'-*TCGCAGCCGTCCA-3' 3'- AGCGTCGGCAGGTTCCCAAA-5'
DS 20/20mer	5'-*TCGCAGCCGTCCAAGGGTTT-3' 3'- AGCGTCGGCAGGTTCCCAAA-5'

Protein.

Klenow was expressed and purified as previously described by Joyce, et al (1983) (7) with modifications as described by Richard (2006) (12). *Klendra* was expressed and purified as previously described by Warfel (2015) (3). *Klentaq* was expressed and purified as previously described by Datta (2003) (13).

Buffers. The buffers shown in Table 2 were used to maintain pH conditions during fluorescence anisotropy titrations. Klenow titrations were performed at higher salt concentration so that its binding affinity would be within the experimentally accessible range of the anisotropy assay.

pH	Klendra and Klentaq	Klenow
5.7-5.9	10mM Acetic Acid 100mM KCl 5mM $MgCl_2$	10mM Acetic Acid 500mM KCl 5mM $MgCl_2$
6.0-6.9	2mM PIPES 100mM KCl 5mM $MgCl_2$	2mM PIPES 500mM KCl 5mM $MgCl_2$
7.0-8.0	10mM Tris 100mM KCl 5mM $MgCl_2$	10mM Tris 500mM KCl 5mM $MgCl_2$

Table 2: Buffer components used in different pH ranges for polymerase binding titrations. This table contains the composition of each buffer used in DNA titrations and the pH and protein with which each buffer was used.

2.2.1: Methods

Fluorescence anisotropy titration. Titrations were performed between pH values of 5.7 and 8. The lowest pH used was pH 5.7, as this is the lowest pH where the fluorescent ROX marker on the DNA substrates remains usable. Below this pH, the ROX label is protonated and will no longer emit a detectable signal. The binding of each protein to both blunt-ended dsDNA (DS 20/20mer) and primed-template ptDNA (PT 13/20mer) was characterized. Measurements were collected on a Horiba Fluoromax-4 spectrofluorometer with FluorEssence V3.5 software.

Data Analysis. Raw anisotropy measurements were normalized by subtracting the initial anisotropy measurement of a sample that contained buffer and DNA substrate but not protein, from the sample anisotropy measurement, and dividing by the largest anisotropy value. Normalized anisotropy was plotted on the y-axis against protein concentration (Klenow, Klendra, or Klentaq) on the x-axis.

The program Kaleidagraph was used to perform linear and non-linear regressions. Klendra and Klentaq titration curves were analyzed with the single-site binding isotherm.

$$Y = n * \frac{[Protein]/K_d}{1 + ([Protein]/K_d)}$$

The Klenow titration curve at pH 5.7 was analyzed with the Hill Equation, because it showed cooperative, sigmoidal character.

$$Y = \frac{[Protein]^{N_H}}{{K_d}^{N_H} + [Protein]^{N_H}}$$

pH linkages were analyzed with a linear fit, where slope equals number of protons taken up or released. pH was plotted on the x-axis against log(1/Kd), referred to as pKd (14,15).

$$pKd = n * pH + pH * pKd$$

Protein concentration determination. Concentrations of protein samples were determined by Bradford assay (BioRad) using a BSA standard. Samples absorbance was measured at 450nm on a Cary-100 spectrophotometer.

Results

3.1.1: Polymerases binding to 13/20 ptDNA

pH-dependent DNA binding was characterized for Klendra, Klentaq, and Klenow polymerases using a fluorescence anisotropy assay (16). Results indicate that all the polymerases bind more tightly as the pH is decreased, and indicated a linked proton uptake upon DNA binding. The pH dependence of Klendra DNA-binding, however, is significantly more pronounced than that of Klentaq or that of Klenow. At pH values near 6.5, the affinity of Klendra for DNA is similar to the affinity of Klentaq at pH values near 8 when binding 20/20 dsDNA. Klendra and Klentaq affinities cannot be compared directly to that of Klenow, because Klenow titrations must be performed at much higher salt concentrations to obtain usable data. However Klenow's affinity for dsDNA versus ptDNA substrates can be compared with the other two polymerases. The data indicates that Klenow consistently has a higher affinity for 13/20 ptDNA at all pH values tested.

The Kd for Klendra binding to 13/20 ptDNA becomes weaker by 507.5 nM (decreasing from 40nM to 508nM) with pH increase across a range of 0.5 pH units, as demonstrated in Figure 3, which shows normalized fluorescence anisotropy titration curves of Klendra binding 13/20 ptDNA. Klentaq binding is tighter than that of Klendra at pH's where the data overlaps, as shown in Figure 4 which depicts normalized Klentaq-13/20 ptDNA binding curves as a function of pH. Binding is tightest at pH 5.7 (18.4 nM) and becomes weaker as pH increases (as weak as 341.0 nM), over a range of 2.3 pH units. Kd's range across 322.6 nM, a smaller range than Klendra's range of Kd's, even though the pH range examined is 4 fold wider. This indicates a greater pH dependence in Klendra.

For the Klenow polymerase, there is less of a decrease in binding affinity across a range of 2.3 pH units than for either of the other polymerases studied, as shown in Figure 5, which shows

normalized Klenow-13/20 ptDNA binding curves. The affinity changes by only 144.1 nM across the examined pH range for Klenow. Binding at pH 6.1 (■) is very similar to, though slightly weaker than binding at pH 6.5 (◆), the reverse of the overall trend. This is an unexpected result when compared to the other polymerases, which exhibited binding that became weaker each time pH was increased, but may simply be due to the experimental error between the less pH dependent Kd values for Klenow. Binding affinity is overall much weaker than shown by Klendra or Klentaq, but this is due to the higher salt concentrations necessary for collecting Klenow data. When compared with other Klenow titrations gathered by Deredge (2004), the binding affinities measured with these titrations were greatly reduced. The pH linkage is also lower for the data from Deredge, as shown in Figure 10, although all Klenow linkages are lower than all Klentaq and Klendra linkages. The data collected by Deredge are more reliable because data was collected to saturation, and the Klenow concentration range encompasses the Kd value (9).

3.1.2: Polymerases binding to 20/20 dsDNA

While Figures 3-5 depict ptDNA binding by the polymerases, Figures 6-8 show binding to dsDNA substrates. A similar trend of decreasing binding affinity as pH increases, as seen in binding ptDNA, was expected to occur when binding dsDNA. The data supports this supposition. For Klendra, as pH increases over 1.25 pH units, the binding affinity for 20/20 dsDNA decreases over a range of 302.7 nM, as shown in Figure 8, which shows normalized curves of Klendra binding 20/20 dsDNA. Overall Klendra's affinity for dsDNA is weaker than its affinity for 13/20 ptDNA, as reported in Figure 6, until pH 6.5, where it begins to display higher affinity for 20/20 dsDNA.

Klentaq again displays a weaker pH dependence when binding dsDNA than Klendra, as it did when binding ptDNA. This is illustrated in Figure 7 which depicts normalized titration curves

of Klentaq binding 20/20 dsDNA. As pH increases over a range of 2 pH units, binding affinity decreases over a range of 118.9 nM. Klentaq affinity for 20/20 dsDNA is consistently weaker than its affinity for ptDNA (Figure 4) across the range of pH's studied.

When binding dsDNA, Klenow again showed weak binding overall, though it still displays the same direction for pH linkage. Klenow's binding affinity for dsDNA decreases over a range of 1027.4 nM as pH increases over a range of 1.8 pH units, as shown in Figure 8, which shows normalized titration curves of Klenow binding 20/20 dsDNA. Klenow's affinity for 20/20 dsDNA is consistently lower than its affinity for ptDNA. The Kd's calculated at pH 6.1, 7.3, and 7.5 are technically unreliable because the concentration of the Kd was not reached during the titration. These Kd's are thus estimated based on data at lower concentrations. At pH 5.7, Klenow appears to have a surprising multi-site binding character not seen at higher pH's. This may indicate one Klenow binding to either end of the dsDNA strand, or could be due to other complicating factors associated with the weak binding by the polymerase due to the storage time after purification. When stored, Klenow displays reduced binding over time, and sometimes displays other anomalous behavior. Reaching saturation, shown by a plateau in the titration curve, indicates that the titration reaction has reached completion. As seen in Figure 8, many of the curves did not plateau. Therefore, confidence in the fitted values of these curves lessens. The previously mentioned titrations by Deredge, though performed with ptDNA and not dsDNA, do suggest that the biding affinities calculated may be artificially weak due to the time that the Klenow was stored (9).

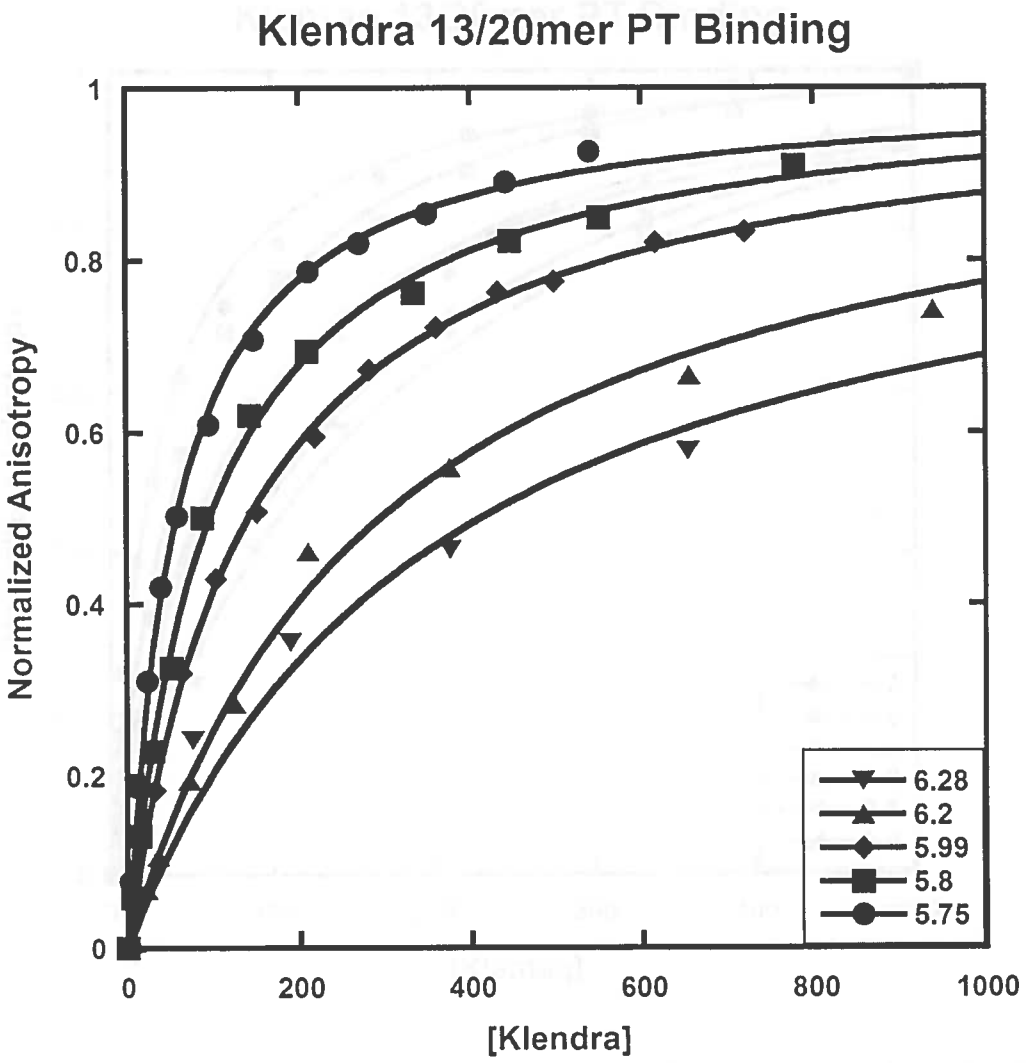

Figure 3: Fluorescence anisotropy titration curves of Klendra binding to 13/20 ptDNA. Normalized anisotropy is on the y-axis versus Klendra concentration in nM on the x-axis. Data were fit with a single-site isotherm equation, as described in Methods. The pH at which each curve was collected is denoted in the inset legend.

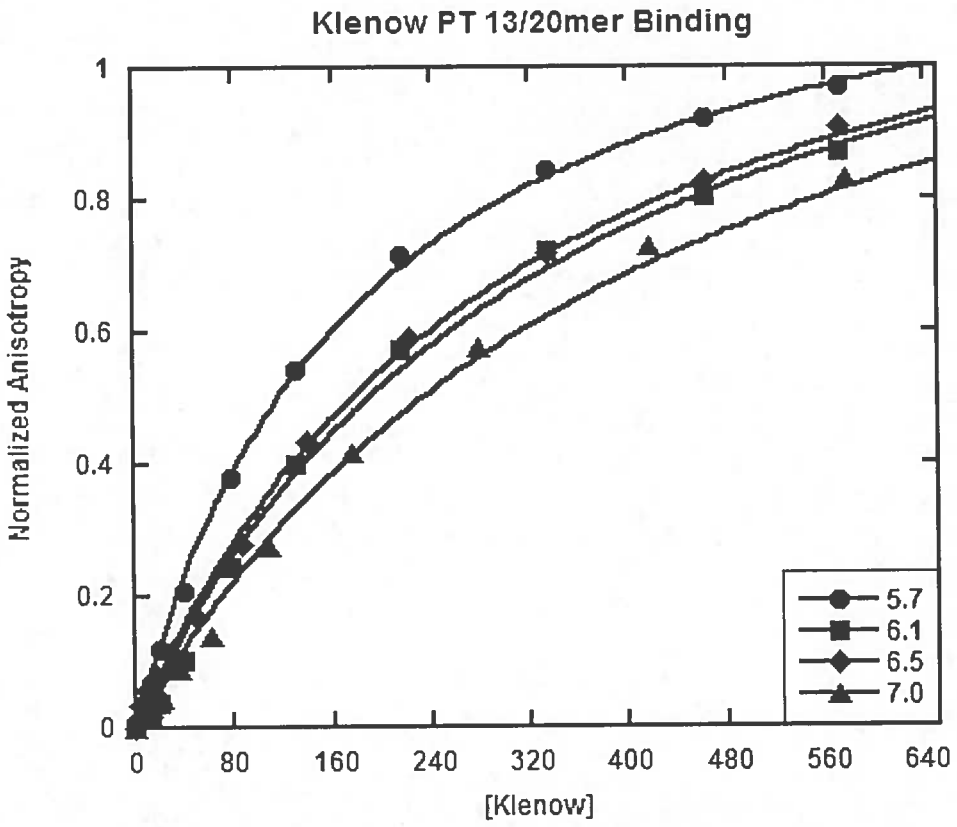

Figure 5: Fluorescence anisotropy titration curves of Klenow binding to 13/20 ptDNA. Normalized anisotropy on the y-axis versus Klenow concentration in nM on the x-axis. Data was fit with the single-site isotherm equation, as described in methods. The pH at which each curve was collected is denoted in the inset legend.

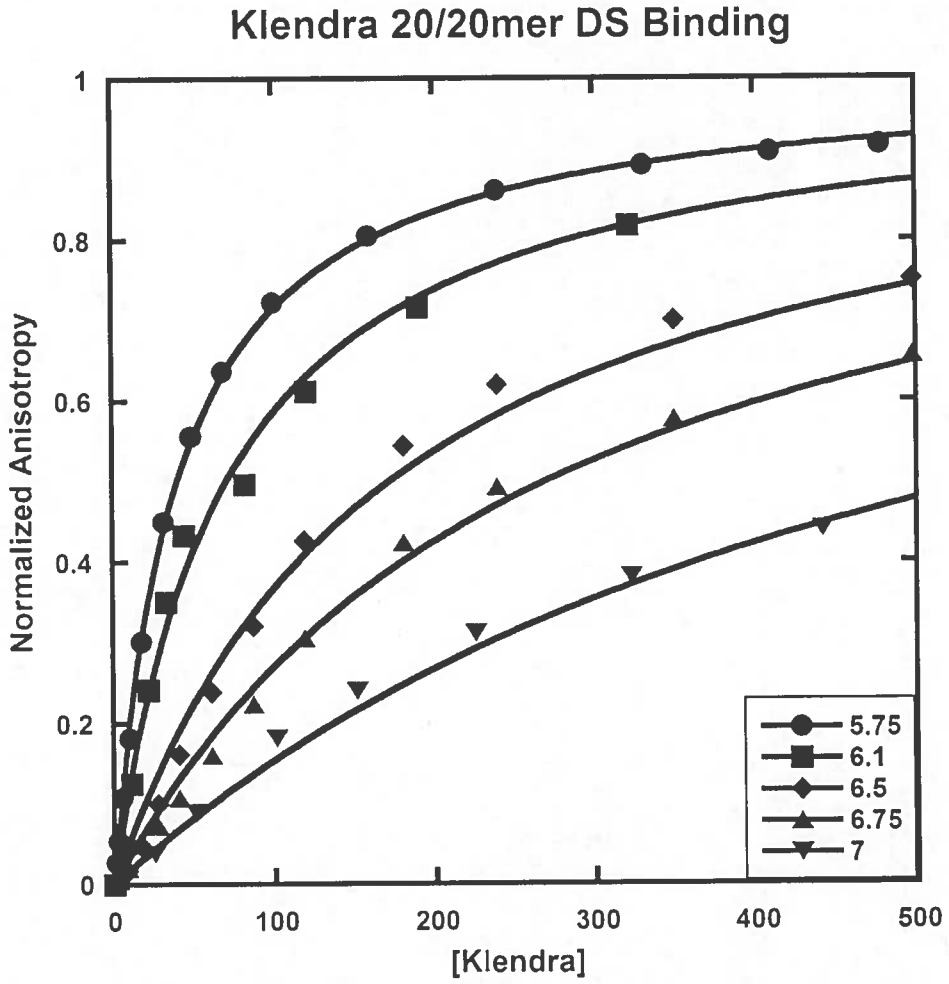

Figure 6: Fluorescence anisotropy titration curves of Klendra binding to 20/20 dsDNA. Normalized anisotropy is on the y-axis versus Klendra concentration in nM on the x-axis. Data were fit with a single-site isotherm equation, as described in Methods. The pH at which each curve was collected is denoted in the inset legend.

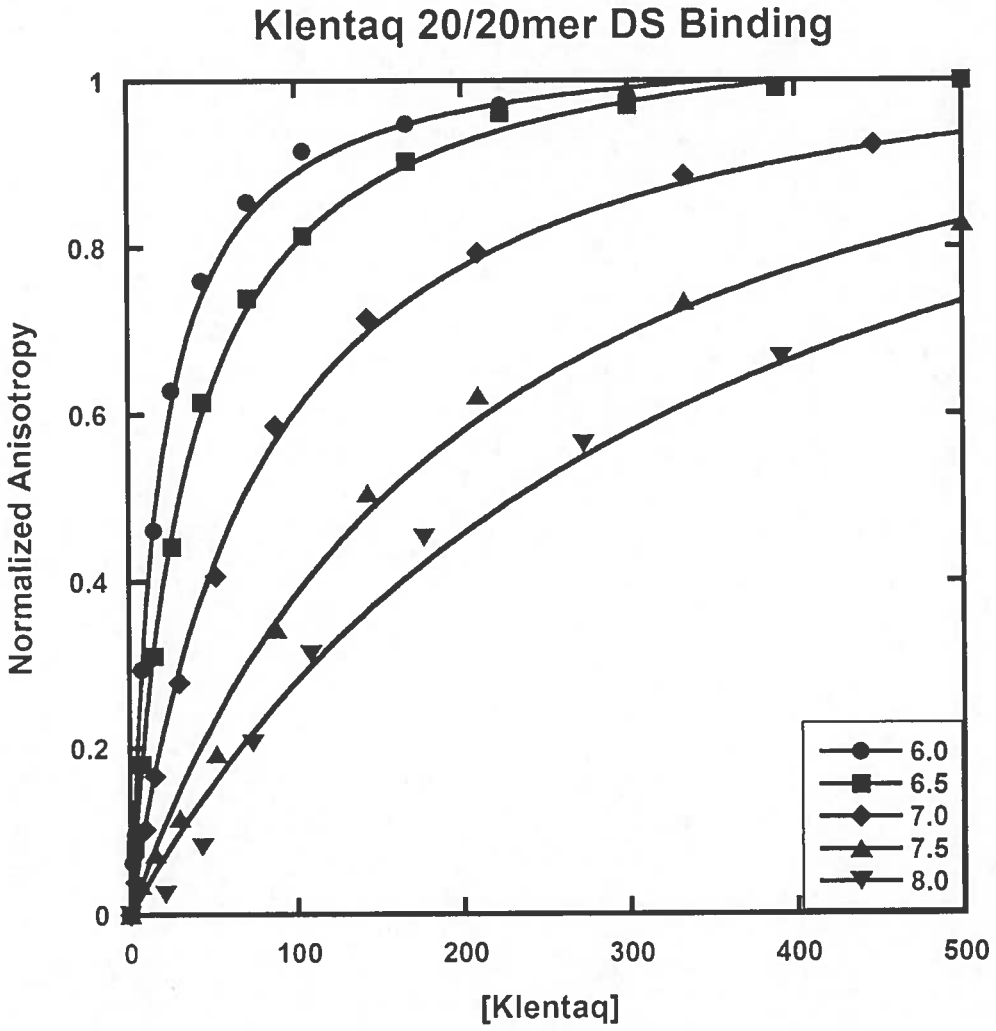

Figure 7: Fluorescence anisotropy titration curves of Klentaq binding to 20/20 dsDNA. Normalized anisotropy is on the y-axis versus Klentaq concentration in nM on the x-axis. Data were fit with a single-site isotherm equation, as described in Methods. The pH at which each curve was collected is denoted in the inset legend.

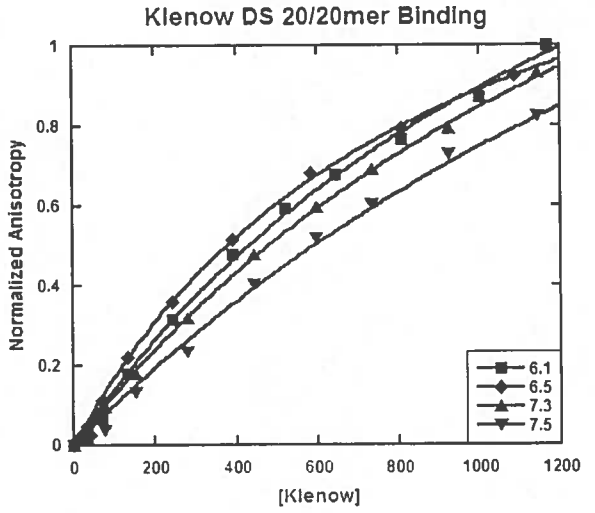

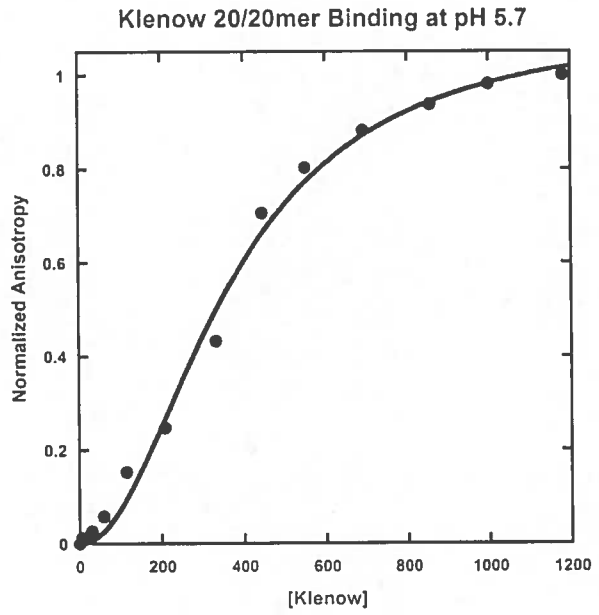

Figure 8: Fluorescence anisotropy titration curves of Klenow binding to 20/20 dsDNA. (A) Normalized anisotropy is on the y-axis versus Klenow concentration in nM on the x-axis. Data were fit with a single-site isotherm equation, as described in Methods. The pH at which each curve was collected is denoted in the inset legend. Kd's fitted at pH 6.1, 7.3, and 7.5 are unreliable because they are outside the data range. **(B)** Fluorescence anisotropy titration curve of Klenow binding 20/20 dsDNA at pH 5.7. Normalized anisotropy is on the y-axis versus Klenow concentration in nM on the x-axis. Titration at pH 5.7 exhibited binding that appeared cooperative, as indicated by its sigmoidal shape. This was the only pH tested at which Klenow showed this character. The curve was fit with the Hill equation with a Kd of 366.67nM and a Hill coefficient of 2.0.

3.2.1: Proton Linkage Analysis

The $\log(1/K_d)$ of each normalized binding curve was plotted versus pH to determine the proton linkage of binding. Since $pH = -\log[H^+]$, we use pKd to denote a similar transformation of the Kd for binding. In other words, pKd is the –log Kd, or log 1/Kd. The slope of the linear fit indicates an uptake or release of protons. All of the polymerases studied show a negative slope, which means, when plotted as shown, an uptake of protons. For comparison, if log(1/Ka) was plotted on the y-axis versus pH on the x-axis, a negative slope would indicate a release of protons. Binding is tighter at high pKd (low Kd). Proton concentration is highest at low pH. Therefore, if binding is tightest where proton concentration is highest, a proton uptake is favorable to binding (14). Linkage analysis of the binding data indicates a proton uptake of about 1.5 protons when Klendra binds 13/20 ptDNA and an uptake of about 1 proton when binding 20/20 dsDNA. Klentaq showed a less pronounced pH linkage, with a proton uptake of about 0.3 protons when binding 13/20 ptDNA and a proton uptake of about 0.7 when binding 20/20 dsDNA. Klenow showed a minimal pH linkage, with an uptake of about 0.3 protons when binding either 13/20 ptDNA or 20/20 dsDNA.

Klendra's pH linkage is consistently higher than Klentaq's, but the difference is most pronounced when binding 13/20 ptDNA, which is the normal substrate for all the polymerases studied in this thesis. Klendra's pH linkage is five-fold higher than Klentaq's for ptDNA binding as compared to a two-fold difference when binding 20/20 dsDNA. There is also an interesting difference in binding affinities. Klendra consistently has a higher affinity for 20/20 dsDNA than 13/20 ptDNA. In contrast, Klentaq has a higher affinity for 20/20 dsDNA at more acidic pH's, but according to the linkage lines in Figure 9 at about pH 7.15 the affinity for 13/20 ptDNA becomes higher.

Klenow consistently exhibited a higher affinity for 13/20 ptDNA than 20/20 dsDNA across all pH's examined. However, it exhibited a slightly higher proton linkage when binding dsDNA (uptake of 0.35) than when binding ptDNA (uptake of 0.25). Figure 10 shows a comparison between Klenow data collected in this study and collected previously by Deredge (9). Compared to the data collected by Deredge (2004), the Kd values from this study are very high (as much as two fold higher at pH 6.5). The linkage determined by this study is also much higher, indicating a four-fold greater uptake of protons than determined by Deredge (9). The data collected by Deredge is more reliable, because titration curves reached saturation. The decreased Klenow affinities observed in this study are likely due to the difference in storage time for the Klenow used for titrations.

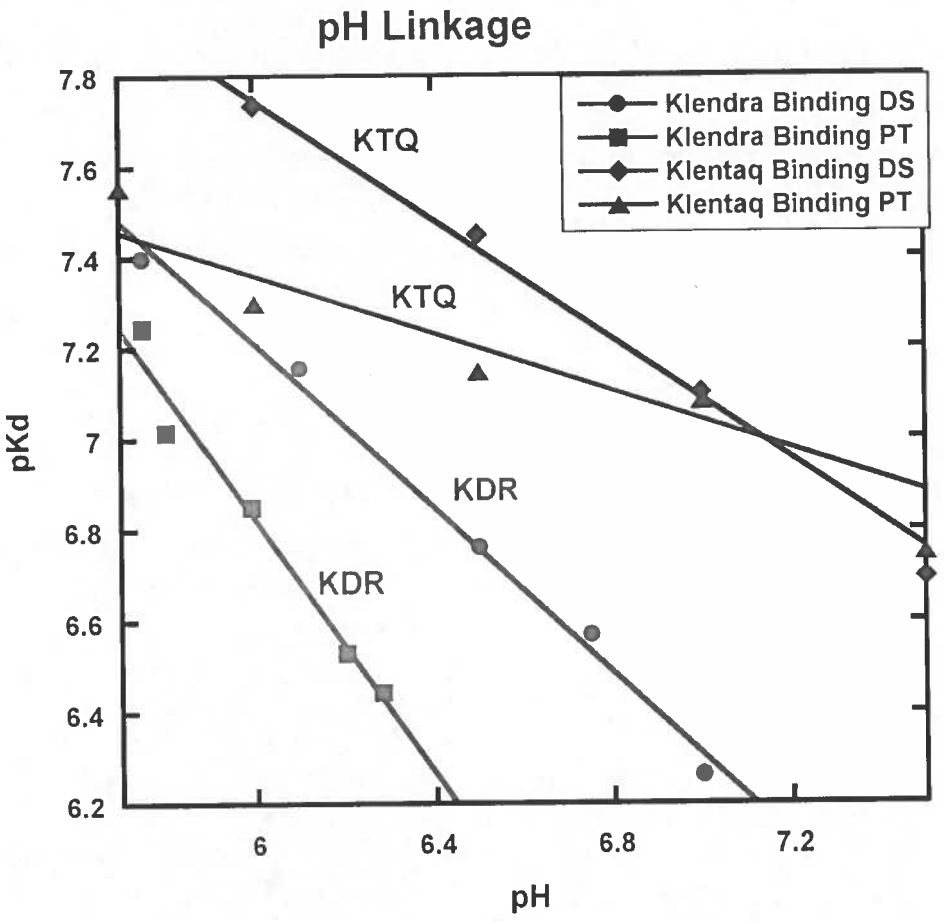

Figure 9: pKd (log ($1/K_d$) or $-\log K_d$) is plotted on the y-axis and its respective pH plotted on the x-axis. Klendra (KDR) and Klentaq (KTQ) binding ptDNA and dsDNA were plotted as described by the inset legend. Data sets were fit linearly according to the pH linkage equation as described in Methods. The negative slope of the fit indicates an uptake of protons, because the tightest binding (highest pKd) is when proton concentration is highest (lowest pH).

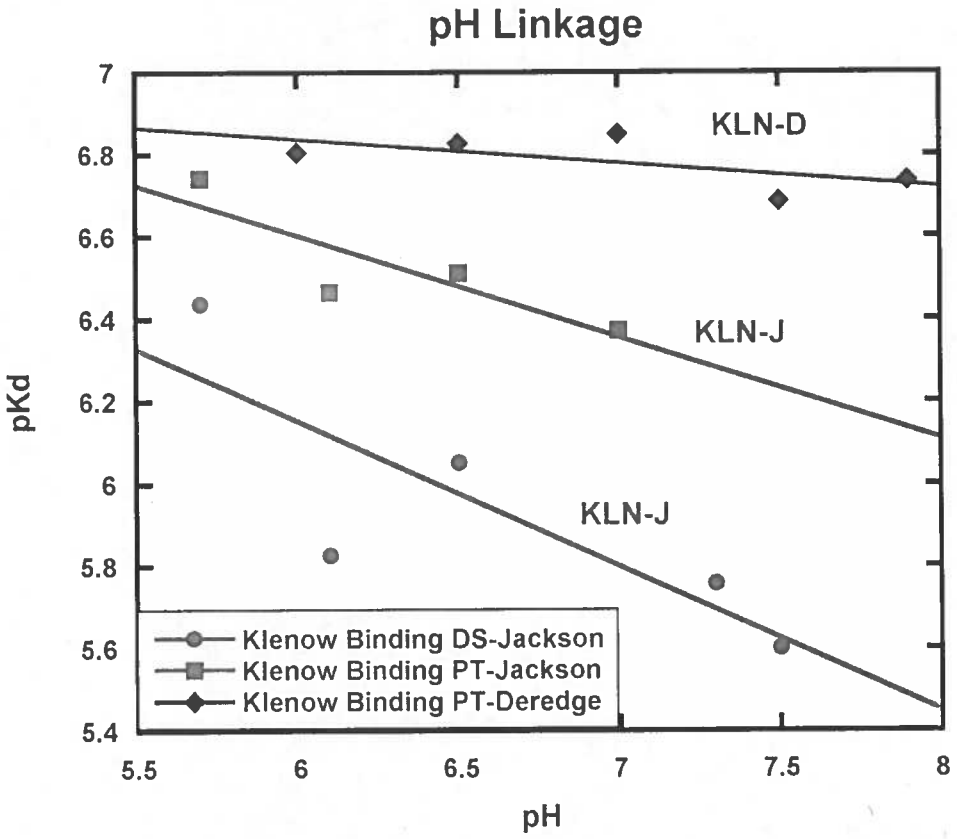

Figure 10: pKd (log ($1/K_d$) or $-\log K_d$) is plotted on the y-axis and its respective pH plotted on the x-axis. Klenow binding data from Deredge (KLN-D) and this study (KLN-J) are plotted. Klenow binding ptDNA and dsDNA were plotted as described by the inset legend. Data sets were fit linearly according to the pH linkage equation as described in Methods. The negative slope of the fit indicates an uptake of protons, because the tightest binding (highest pKd) is when proton concentration is highest (lowest pH).

Table 3: Table of Kd values. Kd's for Klendra, Klentaq, and Klenow are reported for binding 13/20 ptDNA and dsDNA. The smaller the Kd, the tighter the binding.

Table of Kd Values

	PT		DS	
	pH	**Kd**	**pH**	**Kd**
Klendra	5.75	40.4 +/- 1.0	5.75	56.8 +/- 2.0
	5.8	70.0 +/- 5.6	6.1	96.7 +/- 4.6
	5.99	172.7 +/- 16.5	6.5	104.6 +/- 4.0
	6.2	269.0 +/- 17.1	6.75	295.3 +/- 19.3
	6.28	548.0 +/- 33.4	7	359.5 +/- 49.1
Klentaq	5.7	27.8 +/- 1.7	6.0	18.4 +/- 0.93
	6.0	50.2 +/- 3.4	6.5	35.7 +/- 1.1
	6.5	71.4 +/- 3.5	7.0	79.5 +/- 2.5
	7.0	82.9 +/- 1.4	7.5	202.0 +/- 11.2
	7.5	178.2 +/- 11.9	8.0	341.0 +/- 29.0
	8.0	146.7 +/- 7.7		
Klenow	5.7	151.3 +/- 3.8	5.7	366.66 +/- 25.69
	6.1	232.5 +/- 19.2	6.1	1494.3 +/- 194.0
	6.5	278.0 +/- 21.4	6.5	889.2 +/- 33.2
	7.0	295.4 +/- 8.3	7.3	1752.1 +/- 85.1
			7.5	2518.8 +/- 366.7

Table 4: Klenow binding 13/20 ptDNA data collected by D. Deredge, (2004). Binding titrations were performed by D. Deredge at 500mM KCl, as in this study. However, binding is much tighter, likely due to the age of Klenow used.

Klenow 13/20 ptDNA Binding Data, Deredge (9)

pH	Kd (nM)
6	157.2 +/- 11.6
6.5	149.1 +/- 8.8
7	141.5 +/- 21.2
7.5	206.2 +/- 28.9
7.9	183.6 +/- 42.0

Table 5: Table of pH Linkages. pH linkage is determined using the proton linkage equation described in Methods and illustrated in Figures 9 and 10. A positive linkage indicates an uptake in protons.

Table of pH Linkages

	DS 20/20mer	PT 13/20mer
Klendra	0.90	1.40
Klentaq	0.66	0.32
Klenow	0.35	0.25
Klenow (Deredge)	_____	0.06

Discussion

Comparing homologous proteins from different species is an important tool to determine evolutionary relationships and the adaptations that allow the different species to live in their particular environment. Klendra shows a marked pH linkage, though *D. radiodurans* is a neutrophile (17). Klendra's enhanced pH linkage could play an important role in its unique ability to repair and replicate DNA after radiation damage to the genome of *D. radiodurans*. A model for the neutralization of free radicals formed upon irradiation proposed by Daly, et al, hypothesizes that Mn^{++} ions in the cell undergo redox cycling to neutralize free radicals to produce oxygen gas and H^+ ions, a side-effect of which would be lowering the pH of the cell upon irradiation. The hypothesized reactions of this process are illustrated in Figure 13 (1). The affinity data from this study indicates that any resulting drop in pH would result in increased recruitment of Klendra to the DNA where it would be needed for genome protection and repair.

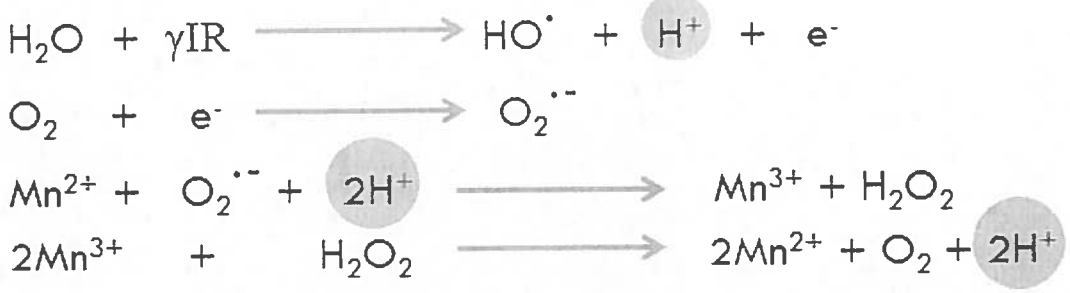

Figure 16: Mn^{2+} Redox cycling inside *D. radiodurans*, as proposed by M. Daly (1). Figure by J. Warfel (3).

The comparison with the closely related Klentaq is informative, and shows that the basic pH linkage for Pol I binding is in the same direction for both polymerases, but that Klendra's linkage is significantly enhanced.

The mesophilic Klenow protein has a lower pH linkage than either extremophile, though the pH linkage is in the same direction as the other polymerases. The linkage determined by Deredge (2004) indicates an even smaller pH linkage than this study. As *E. coli* is not an extremophile or a member of the *Deinococcus-Thermus* group, Klenow's lack of pH linkage is to be expected if pH linkage is an adaptation to extreme environments that arose in the *Deinococcus-Thermus* lineage, but was unnecessary in the *E. coli* lineage.

References

1. Daly, M. J., and Gaidamakova, E. K. (2007) Protein Oxidation Implicated as the Primary Determinate of Bacteria Radioresistance. *PLoS Biol* **5**, 769-779
2. Griffiths, E., and Gupta, R. S. (2004) Distinctive Protein Signatures Provide Molecular Markers and Evidence for the Monophyletic Nature of the Deinococcus-Thermus Phylum. *Journal of Bacteriology* **186**, 3097-3107
3. Warfel, J. (2015) Thermodynamics of DNA Binding by DNA Polymerase I and RecA Recombinase from Deinococcus radiodurans. Doctor of Philosophy, Louisiana State University
4. Beese, L., Friedman, J., and Steitz, T. (1993) Crystal structures of the klenow fragment of DNA polymerase i complexed with deoxynucleoside triphosphate and pyrophosphate. *Biochemistry* **32**, 14095
5. Li, Y., Korolev, S., and Waksman, G. (1998) Crystal structures of open and closed forms of binary and ternary complexes of the large fragment of Thermus aquaticus DNA polymerase I: structural basis for nucleotide incorporation. *The EMBO journal* **17**, 7514-7525
6. Arnold, K., Bordoli, L., Kopp, J., and Schwede, T. (2006) The SWISS-MODEL workspace: a web-based environment for protein structure homology modelling. *Bioinformatics* **22**, 195-201
7. Joyce, C. M., and Grindley, N. D. F. (1983) Construction of a Plasmid That Overproduces the Large Proteolytic Fragment (Klenow Fragment) of DNA Polymerase I of Escherichia coli. *Proceedings of the National Academy of Sciences of the United States of America* **80**, 1830-1834
8. Heinz, K., and Marx, A. (2007) Lesion Bypass Activity of DNA Polymerase A from the Extremely Radioresistant Organism Deinococcus Radiodurans. *The Journal of Biological Chemistry* **282**, 10908-10914
9. Deredge, D. J. (2004) Characterization of the "Glutamate Effect" on the Solution Thermodynamics and Function of the Large Fragments of the Type I DNA Polymerases from E.coli and T.aquaticus. Doctor of Phiolosophy, Louisiana State University
10. Kornberg, A. (1989) The early history of DNA polymerase: a commentaryon 'Enzymic synthesis of deoxyribonucleic acid' by A. Kornberg, I.R. Lehman, M.J. Bessman and E.S. Simms Biochim. Biophys. Acta 21 (1956) 197–198. *Biochimica et Biophysica Acta (BBA) - General Subjects* **1000**, 53-58
11. Johnson, K. A., Bryant, F. R., and Benkovic, S. J. (1984) Continuous assay for DNA polymerization by light scattering. *Analytical Biochemistry* **136**, 192-194
12. Richard, A. J., Liu, C.-C., Klinger, A. L., Todd, M. J., Mezzasalma, T. M., and LiCata, V. J. (2006) Thermal stability landscape for Klenow DNA polymerase as a function of pH and salt concentration. *BBA - Proteins and Proteomics* **1764**, 1546-1552
13. Datta, K., and LiCata, V. J. (2003) Salt dependence of DNA binding by Thermus aquaticus and Escherichia coli DNA polymerases. *Journal of Biological Chemistry* **278**, 5694-5701
14. Record, M. T. J., Lohman, T. M., and De Haseth, P. (1976) Ion effects on ligand nucleic-acid interactions. *Journal of Molecular Biology* **107**, 145-158
15. Coussens, N. P., Schuck, P., and Zhao, H. (2012) Strategies for assessing proton linkage to bimolecular interactions by global analysis of isothermal titration calorimetry data. *The Journal of Chemical Thermodynamics* **52**, 95-107

16. LiCata, V. J., and Wowor, A. J. (2008) Applications of Fluorescence Anisotropy to the Study of Protien-DNA Interaction. *Methods in Cell Biology* **84**, 243-262
17. Slade, D., and Radman, M. (2011) Oxidative stress resistance in Deinococcus radiodurans. *Microbiology and molecular biology reviews : MMBR* **75**, 133-191